SLFN11 inactivation induces proteotoxic stress

and sensitizes cancer cells to ubiquitin activating enzyme inhibitor TAK-243

（SLFN11 の不活性化はタンパク毒性によるストレスを生じ、

ユビキチン活性化酵素阻害剤 TAK-243 に対する腫瘍細胞の感受性を高める）

申 請 者　弘前大学大学院医学研究科

病態制御学領域

消化器内科学教育研究分野

氏　　名　　村 井　康 久

指導教授　　櫻 庭　裕 丈

Abstract

Schlafen11 (SLFN11) inactivation occurs in approximately 50% of cancer cell lines and in a large fraction of patient tumor samples, which leads to chemoresistance. Therefore, new therapeutic approaches are needed to target *SLFN11*-deficient cancers. To that effect, we conducted a drug screen with the NCATS mechanistic drug library of 1978 compounds in isogenic *SLFN11*-knockout (KO) and wild-type (WT) leukemia cell lines. Here we report that TAK-243, a first-in-class ubiquitin activating enzyme UBA1 inhibitor in clinical development, causes preferential cytotoxicity in *SLFN11*-KO cells; this effect is associated with claspin-mediated DNA replication inhibition by CHK1 independently of ATR. Additional analyses showed that *SLFN11*-KO cells exhibit consistently enhanced global protein ubiquitylation, endoplasmic reticulum (ER) stress, unfolded protein response (UPR), and protein aggregation. TAK-243 suppressed global protein ubiquitylation and activated the UPR transducers PERK, phosphorylated eIF2alpha, phosphorylated IRE1, and ATF6 more effectively in *SLFN11*-KO cells than WT cells. Proteomic analysis using biotinylated mass spectrometry and RNAi screening also showed physical and functional interactions of SLFN11 with translation initiation complexes and protein folding machinery. These findings uncover a previously unknown function of SLFN11 as a regulator of protein quality control and attenuator of ER stress and UPR. Moreover, they suggest the potential value of TAK-243 in *SLFN11*-deficient tumors.

Significance

This study uncovers that *SLFN11* deficiency induces proteotoxic stress and sensitizes cancer cells to TAK-243, suggesting that profiling *SLFN11* status can serve as a therapeutic biomarker for cancer therapy.

Introduction

Schlafen11 (SLFN11) drives the cytotoxicity of a wide range of anticancer agents targeting DNA replication: topoisomerase I and II (TOP1 & TOP2) inhibitors, DNA synthesis inhibitors (gemcitabine, hydroxyurea, cytarabine), alkylating agents (cis- and carbo-platin) and poly (ADPribose) polymerase (PARP) inhibitors (talazoparib, olaparib, niraparib, rucaparib) [reviewed in (1)]. SLFN11 is one of the five human Schlafen genes, only found in mammals. SLFN11 is involved in an increasing number of cellular functions including cellular proliferation, DNA replication and native immune response to viral infections (1).

At the molecular level, SLFN11 targets DNA replication by binding to replication forks via replication protein A1 (RPA1) (2,3), blocking the replicative helicase complex (3), inducing the degradation of the replication initiation factor CDT1 (4) and stalled replication forks (5) and causing chromatin opening with activation of the stress response and immediate early response genes (IEGs) (6). Because approximately 50% of cancer cell lines and a large fraction of patient tumors do not express SLFN11 and are resistant to DNA replication-targeted therapies (1,7-15), an unanswered question is how to target *SLFN11*-negative cancer cells.

The medical importance of SLFN11 beyond anti-cancer therapy includes its reported anti-human immunodeficiency virus (HIV) function due to transfer RNA (tRNA) pool alterations and codon-bias discrimination (16). In non-human primates, SLFN11 has also been shown to reduce protein production from the host genes as well as from viral transcripts without codon optimization (17). Recently SLFN11 has been found to directly bind to the ribosomal protein S4 X-linked (RPS4X) and inhibit its function along with the mTOR pathway resulting in suppression of tumor growth and metastasis (14).

The unfolded protein response (UPR) is a homeostatic mechanism in response to the accumulation of unfolded and aggregated proteins in the endoplasmic reticulum (ER) (18). While at least three branches of the UPR including PERK-eIF2α-ATF4, IRE1-XBP1 and ATF6 are well-known, the relationship between

the UPR and DNA replication is unclear. Yet, prolonged and uncontrolled UPR leads to cell cycle arrest and apoptotic cell death (19,20).

Targeting the ubiquitin-proteasome system (UPS) is a recent focus of investigations in preclinical models and clinical trials. The generation of ubiquitin-conjugated proteins in mammals is regulated by two ubiquitin activating (E1) enzymes, UBA1 (also known as UBE1) and UBA6. UBA1 is responsible for >99% of cellular ubiquitin and has a catalytic role in ubiquitin-charging for all E2 ubiquitin-conjugating enzymes (approximately 35) (21).

TAK-243 (initial designation, MLN7243) is a first-in-class inhibitor of the ubiquitin activating enzyme UBA1, in clinical trials as anti-cancer agent. The drug binds free ubiquitin to form a TAK-243–ubiquitin adduct inhibiting UBA1 (22). Consequently, TAK-243 impairs cellular ubiquitin conjugation resulting in proteotoxic stress and ultimately cancer cell death (23-29). Here we report that TAK-243 is more cytotoxic in the absence of SLFN11 in preclinical cancer cell line models. Mechanistically, we found that TAK-243 suppresses DNA replication by activating CHK1 in response to ER stress and UPR, which is related to a new functional role of SLFN11 as protective factor against proteotoxic stress, excessive ubiquitylation and aggregation of cellular proteins, as well as UPR activation.

Materials and methods

Cell lines and reagents

DU145, CCRF-CEM and MOLT4 were obtained from DCTD, DTP (3,30). DMS114, HEK293 and 293T were purchased from ATCC (Virginia, USA). Li-7 was bought from ElabScience (Texas, USA). DU145, HEK293 and 293T cell lines were grown in DMEM medium (11995065; GIBCO) with 10% fetal bovine serum and 1% penicillin-streptomycin. CCRF-CEM, MOLT4, DMS114 and Li-7 cell lines were grown in RPMI medium 1640 (11875093; GIBCO) added with 10% FBS and 1% penicillin-streptomycin at 37ºC in

5%CO_2. Cell lines in this study were passaged about 15 times; all cell lines were tested by MycoAlert™ Mycoplasma Detection Kit (LT07-418; Lonza). Reagents are listed in the Supplementary Table 1.

Generation of SLFN11-Deleted Cells

SLFN11-deleted DMS114 and Li-7 cells were generated by a CRISPR/Cas9 method previously used in DU145, CCRF-CEM and MOLT4 (30).

Cell viability assay

Cells ($2x10^3$ cells) were plated in 96-well white plates (PerkinElmer). After 24-hours incubation, TAK-243 was added and incubated for 72 hours. Cellular viability was determined with ATPlite solution (6016949; PerkinElmer) according to manufacturer's instructions by using an EnVision™ (PerkinElmer).

Western blot analysis

Cells were lysed with RIPA buffer (150 mM NaCl, 50 mM Tris-HCl (pH 7.5), 1 mM EDTA, 1% NP40 (v/v), 0.1% SDS (v/v) and 0.5% sodium deoxycholate (w/v)), protease inhibitor cocktail (Cell Signaling) and phosphatase inhibitor (ThermoScientific). Cell lysates were loaded into wells of Novex tris-glycine gels (Invitrogen) and transferred into Immun-Blot PVDF membranes (BioRad). Membranes were incubated with the indicated primary antibodies (Supplementary Table 1) in 1% milk/PBS-T at 4 °C and subsequently incubated with the horseradish peroxidase (HRP)-conjugated secondary antibodies (NA931 and NA934; GE Healthcare). Protein signals were visualized by ChemiDoc™ Touch MP. Quantification of band intensity was done using ImageJ software and Image Lab software (BioRad).

EdU (5-ethynyl-2'-deoxyuridine) incorporation assay by flow cytometry

Cells were seeded in 6-well plates and treated by drugs, following incubation with EdU 10 μM for 30 min prior to cell harvest. EdU incorporation was measured by Click-iT™ Plus EdU Alexa Fluor™ 647 Flow Cytometry Assay Kit (Invitrogen) according to the manufacturer's protocols. For DNA staining, cells were

mixed with 500 µL of FACS analysis solution containing DAPI. Analysis of the samples was performed by flow cytometry using a FACS Canto (Becton Dickinson) and FlowJo.

Molecular combing assay

Profiling of replication forks was measured by using DNA combing assay as previously described (31). For the analysis of fork elongation speed, CIdU / ldU fibers were picked up randomly. The length of CIdU and ldU were measured and their ratio was calculated. For the analysis of new origin firing, all DNA fibers in one section of each coverslips were counted from captured images. Green-colored single fibers of IdU were defined as new origin firings. Their percentages were calculated by a relative equation.

Immunofluorescence staining analysis

Cells ($5x10^4$ cells) were seeded on chamber slides (Alkali Scientific) and treated with TAK-243. Cells were incubated with 10 µM EdU for 30 min prior to cell harvest. After PBS washing, cells were fixed and permeabilized with 0.3% Triton X-100/PBS for 30 min. Next, cells were incubated with Click-IT Plus reaction cocktail (C10339; Invitrogen) for 30 min followed by washing with PBS and blocking with 3% BSA/PBS-T for 30 min. The cells were incubated overnight with primary antibodies/3% BSA/PBS-T at 4°C. After washing with PBS-T, the cells were incubated with second antibodies/3% BSA/PBST by 1:1000 dilution for 1-2 hours. After washing, cells were mounted with Vectashield with DAPI (H-1200; VECTOR). Images were captured with a Zeiss LSM 780 confocal microscope.

Small interfering RNA transfection

DU145 and its *SLFN11*-KO cells were seeded in a 6-well plate at a density of $2x10^5$ cells/well. Cells were transfected by the Lipofectamine RNAiMax (13778150; Thermo Fisher Scientific) according to the manufacturer's instructions for 48 hours. siClaspin was obtained from Dharmacon (siGENOME Human

Claspin siRNA SMARTPool; M-00528-00-0005). The siRNA sequences of EIF3B and CCT2 are listed in Supplementary Table 1.

BioID pull down and mass spectrometry and validation

SLFN11-BioID2-HA was cloned by PCR with primers (Supplementary Table 1) into MCS-BioID2-HA was a gift from Kyle Roux (74224; Addgene plasmid) by NheI (R0131; NEB) and BspEI (R0540; NEB) restriction enzyme sites (32). HEK293 cells were transiently transfected with empty vector and SLFN11-BioID2-HA by GeneJuice for 48 hours. Cells were incubated with 40 μM biotin (B4501; Sigma) for 24 hours prior to harvest. After PBS wash, cells were lysed in NETN150 buffer (1% NP40, 150 mM NaCl, 0.1 mM EDTA, and 50 mM Tris [pH 7.5]) supplemented with protease inhibitor cocktail. After centrifugation, supernatant was incubated with 100 μL of Dynabeads™ MyOne™ Streptavidin C1 (65001; Invitrogen) for 24 hours. Beads were washed twice with PBS on a magnetic stand. For mass spectrometry, beads were separated by SDS-PAGE gel and analyzed according to previously described protocols (3).

Flow cytometry analysis with L-homopropargylglycine (HPG) labeling and PROTEOSTAT® staining

In HPG labeling, we used a Click-iT™ HPG Alexa Fluor™ 488 Protein Synthesis Assay Kit (C10428; Invitrogen) to measure HPG incorporation with the method based on the manufacture's datasheet and a previous literature (33). In brief, cells were seeded at the density of 3.0×10^5/2 mL with methionine-containing complete RPMI media with FBS. After 24-hours incubation, the cells were washed by pre-warmed PBS and incubated with serum-free RPMI lacking methionine (R7513; Sigma) and HPG 25 μM for 30 min. All cells were harvested with EDTA-trypsin and fixed in PBS with 4% PFA for 15 min on ice. Next, cells were permeabilized in 100 μL of PBS containing 0.1% saponin for 15 min at room temperature and then re-suspended with 250 μL of Click-iT reaction cocktails and incubated for 30 min. The pellets were washed twice and transferred with PBS into 5 mL FACS tubes. FITC fluorescence signal was measured by flow cytometry using a FACS Canto (Becton Dickinson).

In PROTEOSTAT® staining, we used a PROTEOSTAT® Aggresome detection Kit (ENZ-51035; Enzo) to measure misfolded and aggregated proteins using the method provided by the manufacture. In brief, cells were incubated in complete media with FBS for 24 hours and harvested with EDTA-trypsin. Next, cells were mixed with 4% PFA-based fixative solution for 30 min, permeabilized in 0.5% triton X-100-based permeabilization solution for 30 min at room temperature, and then re-suspended with 500 μL of PROTEOSTAT® aggresome red detection reagent using fresh dilution of ENZ-51035-0025 by 1,500 fold. After one-hour incubation, the mixture was transferred into 5 mL FACS tubes. The fluorescence signal was measured by PI channel of the FACS Canto.

Quantification and statistical analysis

All statistical analyses were conducted with GraphPad Prism9.0. Statistical significances were determined by the unpaired t test (Figure 1E, 5I, S5C, S5F, S5H, 6A and 6B), the two-way ANOVA test (Figure S1D, 2B, S2B, 3B, 4B, 4E, S4H and S4J), the ordinary one-way ANOVA test (Figure 2D, 2F, 2G, S2C, S2D, 3F, 3I, 4G, 4H and 5C), Sidak's multiple comparisons test (Figure S1D, 2D, 4E and S4J) and Tukey's multiple comparisons test (Figure 2B, 2F, 2G, S2B, S2C, S2D, 3B, 3C, 3F, 3I, 4B, 4G, 4H, S4H and 5C). The threshold for statistical significance was $P < 0.05$. For the quantitative data, the statistical parameters were shown in the figure legends.

The rest of Materials and Methods are described in Supplementary Data.

Results

TAK-243 causes selective cytotoxicity in *SLFN11*-deficient cancer cells.

To detect therapeutic compounds selective for *SLFN11*-negative cells, we performed a highthroughput drug screening in isogenic leukemic lymphoblast cell lines, CCRF-CEM *SLFN11* wild-type (WT) and *SLFN11*

knockout (KO) (3). As expected, topoisomerase inhibitors, well-known DNA damaging agents, showed increased cytotoxicity in *SLFN11*-WT cells than *SLFN11*-KO cells (Figure 1A) (3,15). Conversely, TAK-243 induced greater cytotoxicity towards *SLFN11*-KO cells (Figure 1A and S1A).

To confirm the selective cytotoxicity of TAK-243 in *SLFN11*-KO cell lines, we tested three isogenic cancer cell line pairs expressing SLFN11 and their *SLFN11*-KO counterparts: prostate cancer DU145, hepatocellular carcinoma Li-7 and leukemic lymphoblasts MOLT4. While the DU145 and MOLT4 cell lines were previously reported (30), the Li-7 *SLFN11*-KO cells were generated by CRISPR/CAS9 for the present study (Figure S1B) and were confirmed to be resistant to CPT (Figure S1C). In all three pairs of cell lines, *SLFN11*-KO cells were significantly more sensitive to TAK-243 than their WT counterparts (Figure 1B-D). Figure 1E summarizes the differential TAK-243 activity for the three pairs of isogenic *SLFN11*-expressing and KO cell lines. The sensitivity difference to TAK-243 between the *SLFN11*-WT and KO cells was confirmed by clonogenic assays. Colony formation in *SLFN11*-KO cells was significantly reduced at the concentration of 50 nM ($p < 0.05$) compared to WT cells (Figures 1F and S1D).

TAK-243 also caused more apoptotic cell death in the *SLFN11*-KO cells compared to *SLFN11*-WT cells (Figure S1E). In addition, the annexin V-negative and PI-positive population was increased in the *SLFN11*-KO cells, indicating that TAK-243 caused some necrotic cell death. Apoptotic cell death in *SLFN11*-KO cells was validated as increased cleaved PARP and cleaved caspase-3 (Figure S1F). These results show that TAK-243 preferentially suppresses cell viability of *SLFN11*-deficient cancer cells, suggesting that UBA1 activity fosters the survival of *SLFN11*-KO cells.

TAK-243 inhibits DNA synthesis more effectively in *SLFN11*-deficient than proficient cancer cells.

We next examined DNA replication in response to TAK-243 treatment because SLFN11 is well established to inhibit DNA replication in response to replication stress (1,3,5,6). We first performed pulse incorporations of the thymidine analog 5-ethynyl-2'-deoxyuridine (EdU) in *SLFN11*-WT and -KO cells treated with TAK-243 to evaluate DNA synthesis. TAK-243 decreased EdU incorporation within 4 hours

significantly more in *SLFN11*-KO than in *SLFN11*-WT cells (Figure 2A-B). EdU incorporation was inhibited by more than 80% after 0.5 μM TAK-243 in the *SLFN11*-KO cells while it was inhibited less than 20% in the *SLFN11*-WT cells (Figure 2A). The reduced EdU incorporation was observed over 24 hours with a lower concentration of TAK-243 (Figure S2A-B). To confirm the FACS results, immunofluorescence staining was performed after EdU pulse-labeling. *SLFN11*-KO cells showed enhanced loss of EdU staining after TAK-243 treatment (Figure 2C-D). These results show that TAK-243 suppresses DNA synthesis more effectively in *SLFN11*-KO cells than *SLFN11*-WT cells.

To analyze the effects of TAK-243 on DNA replication at the molecular level, we measured fork elongation and replication origin firing using molecular combing (31). *SLFN11*-WT and -KO cells were incubated with chlorodeoxyuridine (CIdU; red) for 1 hour and then treated with TAK-243 and iododeoxyuridine (IdU; green) for 2 hours (Figures 2E and S2C-D). The ratio of IdU/CIdU represents fork elongation speed with an expected value of 2 in the absence of drug treatment (Figure 2F). The IdU/CldU ratio was significantly decreased in *SLFN11*-KO cells treated with TAK-243, indicating that TAK-243 reduces replication fork speed more effectively in *SLFN11*-KO cells (Figure 2E-F and S2C-D). In the same experiments, we also analyzed the ratio of IdU single-colored fibers versus the total measured fibers to estimate new origin firing (Figure 2G). *SLFN11*-KO cells treated with TAK-243 showed significantly less origin firing compared to *SLFN11*-WT cells or untreated cells. These results show that TAK-243 interrupts DNA replication both at the fork elongation and origin firing levels most effectively in *SLFN11*-KO cells.

TAK-243 blocks DNA synthesis through CHK1 activation via Claspin, but independently of ATR in *SLFN11*-KO cells.

To determine how TAK-243 suppresses DNA replication, we evaluated the phosphorylation of DNA damage response (DDR) signaling molecules. Under conditions where TAK-243 induced cellular DNA replication inhibition, we observed increased phosphorylation of CHK1 (S345) in the *SLFN11*-KO cells (Figure 3A and 3B). CHK1 hyperphosphorylation was also detected in the *SLFN11*-KO cells 10 hours at

lower concentrations of TAK-243 (Figure S3A). Notably, in contrast to CPT, which was used as a positive control (31), CHK1 activation by TAK-243 was not accompanied by phosphorylation of RPA2 and γ-H2AX (Figure 3A and S3A), suggesting that TAK-243-induced CHK1 activation is independent of ataxia telangiectasia and RAD3-related (ATR). We confirmed that TAK-243 did not induce detectable ATR activation, which is involved in DDR and is responsive to CPT (Figure 3A, 3C and S3A) (31). Additionally, given that CHK1 is generally activated by ATR (34), we tested the effect of an ATR inhibitor on CHK1 activation by TAK-243. Consistent with the lack of ATR activation by TAK-243, the ATR inhibitor M4344 did not suppress the activation of CHK1 by TAK-243 (Figure 3D and 3E) whereas it blocked ATR activation in the case of CPT (Figure S3B). These data suggest that CHK1 activation by TAK-243 is independent from ATR and different from the classical RPA2-ATR-CHK1 activation by CPT (31).

Because Claspin is a mediator of CHK1 activation (35), and because a recent study showed that thapsigargin, an ER stressor, induces CHK1 activation via Claspin and independently of ATR (36), we hypothesized that CHK1 activation by TAK-243 could be mediated by Claspin independently of ATR. To test this hypothesis, we depleted endogenous Claspin using small interfering RNA (siRNA) prior to TAK-243 treatment. Depletion of Claspin in *SLFN11*-KO cells completely blocked the phosphorylation of CHK1 by TAK-243 (Figure 3F), consistent with the role of Claspin as a mediator of CHK1 activation by TAK-243.

To examine this possibility further, we tested whether CHK1 inhibition could restore DNA replication in TAK-243-treated cells. *SLFN11*-KO cells treated with both TAK-243 and the CHK1 inhibitor (LY2606368; prexasertib) showed higher EdU incorporation compared to those treated with TAK-243 alone (Figure 3G-H), indicating that replication inhibition by TAK-243 is mediated by CHK1 activation.

To determine whether CHK1 activation by TAK-243 could be affected by re-expression of SLFN11 in *SLFN11*-deficient cells, we used 293T *SLFN11*-deficient cells (16) transiently transfected with SLFN11-WT expressing construct. Re-expression of SLFN11 in *SLFN11*-deficient cells suppressed TAK-243-induced CHK1 activation (Figure 3I). Together, these results show that TAK-243 suppresses DNA synthesis by activating CHK1 via Claspin independently of ATR.

TAK-243 induces ER stress and UPR more effectively in *SLFN11*-deficient than proficient cells.

TAK-243 is known to induce ER stress and the UPR (22,23,26-29), and the UPR has been shown to activate CHK1 and inhibit DNA replication (36-38). Also, the activation of PERK-eIF2α pathway by thapsigargin or dithiothreitol has been reported to promote the phosphorylation of CHK1 via Claspin independently of ATR (36).

To test whether *SLFN11*-KO cells exhibit increased ER stress and uncontrolled UPR, we probed the three classical pathways associated with the UPR (Figure 4A) (18,39) in DU145 WT and *SLFN11*-KO cells treated with TAK-243 (Figure 4B). Phosphorylated PERK was detected as an electrophoretically upper-shifted band both in *SLFN11*-WT and -KO cells treated with TAK-243. However, the basal level of phosphorylated eIF2α was higher in *SLFN11*-KO cells and more effectively induced by TAK-243 in *SLFN11*-KO than in WT cells (Figure 4B-C). Probing the second IRE1-XBP1 signaling branch of the UPR showed that IRE1 was phosphorylated faster in the *SLFN11*-KO cells than WT cells. Testing the third UPR pathway also showed that ATF6 was increased in both of *SLFN11*-WT and KO cells; however, the baseline expression of ATF6 was higher in the *SLFN11*-KO cells. We confirmed these results in the leukemia CCRF-CEM cells treated for 2 hours (Figure S4A) and in DU145 cells and small cell lung cancer DMS114 cells treated with lower TAK-243 concentrations for 24 hours (Figure S4B-C). Together these experiments show that *SLFN11*-KO cells have enhanced UPR activation both the absence and presence of TAK-243.

To examine whether phosphorylation of CHK1 (S345) by TAK-243 was dependent on the activation of PERK-ATF4 branch, we treated DU145 *SLFN11*-KO cells with TAK-243 and the PERK inhibitor ISRIB. ISRIB significantly blocked the phosphorylation of CHK1 in response to TAK-243 (Figure 4D-E). In addition, consistent with the reported accumulation of short-lived proteins including c-Jun and c-Myc upon TAK-243 treatment (22), we found enhanced accumulation of c-Jun and c-Myc in *SLFN11*-KO cells in response to TAK-243 (Figure S4D), suggesting that *SLFN11*-KO cells treated with TAK-243 have more global protein accumulation. We also tested the cytotoxicity of the p97 inhibitors, NMS-873 and CB5083

in DU145 *SLFN11*-WT and -KO cells because these drugs also induce robust UPR (20). *SLFN11*-KO cells were more sensitive to both p97 inhibitors than WT cells (Figure S4E-F).

Because our data show that *SLFN11*-KO cells demonstrate enhanced UPR response to TAK-243, which primarily acts as an E1 inhibitor, we measured ubiquitin conjugates in *SLFN11*-WT and -KO cells. Notably, the overall baseline levels of ubiquitin conjugates were different in the *SLFN11*-WT and -KO cells. Higher ubiquitin conjugates [(Ub)n] were consistently observed both in the DU145 and CEM *SLFN11*-KO than *SLFN11*-WT cells (Figures 4F and S4G), indicating that lack of SLFN11 enhances global ubiquitylation. After TAK-243 treatment, DU145 *SLFN11*-KO cells lost ubiquitin conjugates in a dose-dependent manner to a greater extent than the *SLFN11*-WT cells. This effect was not related to different UBE1 protein level. Repeated experiments (N = 6) confirmed high levels of ubiquitin conjugates in *SLFN11*-KO cells at a steady-state and more robust reduction of ubiquitin conjugates by TAK-243 in *SLFN11*-KO than WT cells (Figure 4G). Comparable results were obtained in CCRF-CEM *SLFN11*-WT and -KO cells treated for 1 hour with TAK-243 (Figure S4G-H) and in DU145 *SLFN11*-WT and -KO cells treated with TAK-243 at lower concentrations for 24 hours (Figure S4I-J). These results demonstrate that TAK-243 depletes ubiquitin conjugates more effectively in the absence of SLFN11. To confirm that the presence of SLFN11 influences the global ubiquitination at the steady-state condition, we generated doxycycline (Dox)-inducible SLFN11-expressing cells. 72-hour exposure to Dox induced robust SLFN11 expression and significantly reduced global cellular ubiquitination by 40-50% (Figure 4H-I). Together, these results show that cells lacking SLFN11 have increased UPR and ubiquitylation, and that TAK-243 suppresses ubiquitin conjugates and increases UPR and ER stress along with CHK1 activation to a greater extent in *SLFN11*-KO than *SLFN11*-WT cells.

SLFN11 protects cells from UPR by interacting with protein folding and translation initiation complexes.

To test whether absence of SLFN11 leads to an accumulation of misfolded protein, we evaluated aggregated and newly synthesized proteins by PROTEOSTAT® staining and L-homopropargylglycine (HPG) labelling, respectively (Figure 5A and S5A). *SLFN11* WT cells showed less aggregated proteins than KO cells at steady-state condition and TAK-243 increased aggregated proteins in both WT and KO cells (Figure 5B-C). In addition, newly synthesized proteins were less in Li-7 *SLFN11* WT cells than KO cells (Figure S5B-C). These data suggest that SLFN11 can decrease aggregated protein and/or newly synthesized protein at steady-state conditions, which is consistent with the lower levels of ubiquitin conjugates in SLFN11-expressing cells.

Next, to determine whether SLFN11 interacts with protein homeostasis and UPR pathways, we performed proteomic analysis with biotinylated mass-spectrometry (Figure 5D) (32). HEK293 *SLFN11*-proficient cells were transfected with a proximity-dependent biotin identification (BioID)2-fusion empty vector or BioID2-fusion SLFN11. Upon addition of biotin, proteins in close proximity to SLFN11 were biotinylated inside cells. The biotinylated proteins were captured by streptavidin beads and analyzed via mass-spectrometry. As shown in Figure 5E and Supplementary Table 2, TCP1, CCT2, CCT3, CCT4, CCT5, CCT6A, CCT7 and CCT8, which belong to the T-complex protein-1 ring complex (TRiC) and chaperonin containing TCP-1 complex (CCT) in protein folding were identified in *SLFN11*-BioID transfected cells. In addition, translation initiation complex proteins (EIF3A, EIF3B, EIF3D, EIF3E, EIF3F, FIF3H, EIF3L, EIF3M, EIF4B and EIF4G1) were also enriched in *SLFN11*-BioID transfected cells. Gene ontology (GO)-term enrichment analysis with the top 100 hits in the list of biotinylated mass-spectrometry proteins showed translation initiation and protein folding-related pathways as prominent protein networks with SLFN11 (Figure 5F and S5D).

To validate the mass spectrometry data, we performed pull-down experiments with the *SLFN11*-HA-BioID2 construct, and confirmed enrichment of EIF3B, EIF3L and CCT2 in SLFN11-mediated immunoprecipitation (Figure 5G and S5E-F). The interaction of SLFN11 with EIF3B and CCT2 were detected regardless of TAK-243 treatment (Figure 5G). We also validated SLFN11 interaction with EIF3B

and CCT2 by proximity ligation assay (PLA) in DU145 cells (Figure 5H-I). Depletion of the TRiC/CCT chaperonin complex genes (CCT6A, CCT4, TCP1, CCT7, CCT3 and CCT2) consistently showed a greater sensitivity of the *SLFN11*-KO than *SLFN11*-WT cells (Figure S5G and Supplementary Table 3). Additional experiments confirmed that *SLFN11*-KO cells were significantly more dependent on CCT2 than *SLFN11*-WT cells (Figure S5H).

Collectively, these results suggest that SLFN11 plays a role in promoting protein homeostasis and in reducing cellular ubiquitination caused by misfolded proteins.

Discussion

Ubiquitin conjugation and ER stress associated protein degradation (ERAD) by the proteasome are critical for the clearance of misfolded proteins following their cytoplasmic retro-translocation from the ER (40). By blocking the ubiquitin activating enzyme (UBA1), TAK-243 induces irresolvable ER stress and UPR activation (22,26-29). Our data are consistent with the potent and rapid effects of TAK-243 in inhibiting ubiquitin conjugation as visualized by the rapid depletion of cellular polyubiquitylated proteins, especially in *SLFN11*-KO cancer cells. Our study also shows that the activation of UPR by TAK-243 arrests replication within 2 - 4 hours by activating CHK1 as well as by inducing apoptosis and cell death at later time points. Hence, our data support the mechanism of action of TAK-243 and its preferential antiproliferative effects in *SLFN11*-KO cancer cells. They are relevant to the reported activity of TAK-243 in patient-derived xenograft (PDx) models (22,24,26-29), and in the context of the ongoing clinical trials of TAK-243 as first-in-class UBA1 inhibitor (NCT03816319 and NCT02045095).

Our flow cytometry, immunofluorescence microscopy and molecular combing analysis show that TAK-243, in addition to targeting UPR, interrupts replicative DNA synthesis within 2 - 4 hours as it depletes global cellular ubiquitylation. We demonstrate that this replication inhibition is related to CHK1 activation via Claspin without detectable ATR-mediated DDR activation (Figure 6). Consistent with our results, two prior studies reported that TAK-243 itself does not cause DNA damage, and that the

combination of TAK-243 with UV or gamma irradiation suppresses DNA damage repair (22,26). The lack of γ-H2AX induction by TAK-243 in our study can be reconciled with a previous report showing that diffuse large B-cell lymphoma (DLBCL) cells treated with TAK-243 generate γ-H2AX (27). Our interpretation is that the γ-H2AX induction by TAK-243 in the prior study (27) is related to cell death by apoptosis as γ-H2AX is both a marker of DDR and of apoptotic response (41,42). Our finding that TAK-243 arrests DNA replication by activating CHK1 is consistent with independent reports showing that ER stress and uncontrolled UPR cause non-ATR mediated CHK1 activation (36-38).

An unexpected finding is that SLFN11 attenuates the UPR (Figure 6). Indeed, in two different isogenic cell line models (DU145 prostate cancer and CCRF-CEM leukemia), cells expressing SLFN11 showed significantly lower level of global polyubiquitylation at the steady-state condition, along with attenuated baseline of UPR activity and reduced protein aggregation. Our proteomic analysis identifies potential molecular insights for this novel proteostasis activity of SLFN11, as we observed SLFN11 binding to protein folding and translation initiation factors. Profiling of gene dependencies by a genome-wide RNAi screen also supports that *SLFN11* deficient cells are highly dependent on the protein chaperonin and folding genes, implying that absence of SLFN11 leads to protein mis-folding and dependency on cellular ubiquitination, which is inhibited by TAK-243 (Figure 6).

Consistent with the activity of SLFN11 on translation, SLFN11 has been shown to bind type II tRNA leading to its activity as restriction factor against HIV-1 (16) and to cleave type II tRNAs resulting in ATR and ATM inhibition in response to DNA damage (43). SLFN11 has also been reported to limit the infectivity of flaviviruses by targeting host tRNAs (44). Binding and cleavage of tRNAs have also been demonstrated for SLFN13, the close relative SLFN11 (33). Non-human primate SLFN11 also suppresses protein production from viral, non-viral and host transcripts (17). In addition, a recent study showed that SLFN11 suppresses tumor growth and metastasis by inhibiting the RPS4X and mTOR pathway (14).

Our study is also the first to report a potential implication of SLFN11 with protein folding. This finding is plausible with the fact that murine Slfn1 binds to DnaJB6, one of the chaperone proteins of the DnaJ/Hsp

(heat-hock protein) family, leading to the stabilization of Hsp70 (45), which plays an important role in protein folding and protein quality control (46). This complex leads to the localization of Slfn1 to the nucleus and induction of cell cycle arrest and quiescence of murine T cells (45). Additional reports showed that mutation of Slfn2 causes a loss of murine immune cell quiescence and chronic ER stress (47,48). Further studies are warranted to explore the detailed molecular connections between SLFN11, proteostasis and control of ER stress and UPR.

Beyond cancer, uncontrolled ER stress in human cells can induce multiple diseases such as atherosclerosis, diabetes, and neurodegenerative disease including Alzheimer's and Parkinson's disease (49). In addition, the chaperonin TRiC/CCT has been detected as a key molecule protecting cells from amyloid-like protein misfolding (50). Our mass spectrometry analysis showed TCP1 and CCTs as the SLFN11 interactors. Recently, a detailed immunohistochemistry and RNA expression study showed that SLFN11 is expressed in normal human brain cells and other organic cells (12). Our results that *SLFN11*-deficient cells are highly dependent on CCT genes, imply abnormality in the protein folding process in the absence of SLFN11. Taken together, these data suggest that SLFN11 might be involved in protecting normal human cells, especially brain and immune cells, from proteotoxicity, and that malfunction of SLFN11 might be associated with various human diseases including neurodegenerative and autoimmune diseases.

Future investigations are warranted to test our results in *in vivo* xenograft with cell lines and patient-derived models. Our findings may also be relevant for the therapeutic development of TAK-243 with the inclusion of SLFN11 expression as a treatment response predictive biomarker for cancer patient selection. Approximately, 50% of cancer cells do not express SLFN11 (1), therefore TAK-243 may be a therapeutic option for those cancer patients whose tumors are *SLFN11*-negative and do not respond to DNA damaging agents.

Acknowledgement

This project was supported by the Intramural Program, Center for Cancer Research of the National Cancer Institute, NIH (to Yves Pommier): Z01-BC006150. We appreciated all the staff at NCATs for their contribution in this study.

References

1. Murai J, Thomas A, Miettinen M, Pommier Y. Schlafen 11 (SLFN11), a restriction factor for replicative stress induced by DNA-targeting anti-cancer therapies. Pharmacol Ther **2019**;201:94-102
2. Mu Y, Lou J, Srivastava M, Zhao B, Feng XH, Liu T*, et al.* SLFN11 inhibits checkpoint maintenance and homologous recombination repair. EMBO Rep **2016**;17:94-109
3. Murai J, Tang SW, Leo E, Baechler SA, Redon CE, Zhang H*, et al.* SLFN11 Blocks Stressed Replication Forks Independently of ATR. Mol Cell **2018**;69:371-84 e6
4. Jo U, Murai Y, Chakka S, Chen L, Cheng K, Murai J*, et al.* SLFN11 promotes CDT1 degradation by CUL4 in response to replicative DNA damage, while its absence leads to synthetic lethality with ATR/CHK1 inhibitors. Proc Natl Acad Sci U S A **2021**;118
5. Okamoto Y, Abe M, Mu A, Tempaku Y, Rogers CB, Mochizuki AL*, et al.* SLFN11 promotes stalled fork degradation that underlies the phenotype in Fanconi anemia cells. Blood **2021**;137:336-48
6. Murai J, Zhang H, Pongor L, Tang SW, Jo U, Moribe F*, et al.* Chromatin Remodeling and Immediate Early Gene Activation by SLFN11 in Response to Replication Stress. Cell Rep **2020**;30:4137-51 e6
7. Barretina J, Caponigro G, Stransky N, Venkatesan K, Margolin AA, Kim S*, et al.* The Cancer Cell Line Encyclopedia enables predictive modelling of anticancer drug sensitivity. Nature **2012**;483:603-307
8. Buettner R. Awakening of SCHLAFEN 11 by immunohistochemistry: a new biomarker predicting response to chemotherapy. Virchows Archiv **2021**
9. Kagami T, Yamade M, Suzuki T, Uotani T, Tani S, Hamaya Y*, et al.* The first evidence for SLFN11 expression as an independent prognostic factor for patients with esophageal cancer after chemoradiotherapy. BMC Cancer **2020**;20:1123

10. Knelson EH, Patel SA, Sands JM. PARP Inhibitors in Small-Cell Lung Cancer: Rational Combinations to Improve Responses. Cancers (Basel) **2021**;13

11. Moribe F, Nishikori M, Takashima T, Taniyama D, Onishi N, Arima H*, et al.* Epigenetic suppression of SLFN11 in germinal center B-cells during B-cell development. PLoS One **2021**;16:e0237554

12. Takashima T, Sakamoto N, Murai J, Taniyama D, Honma R, Ukai S*, et al.* Immunohistochemical analysis of SLFN11 expression uncovers potential non-responders to DNA-damaging agents overlooked by tissue RNA-seq. Virchows Arch **2020**

13. Winkler C, Armenia J, Jones GN, Tobalina L, Sale MJ, Petreus T*, et al.* SLFN11 informs on standard of care and novel treatments in a wide range of cancer models. Br J Cancer **2020**

14. Zhou C, Liu C, Liu W, Chen W, Yin Y, Li CW*, et al.* SLFN11 inhibits hepatocellular carcinoma tumorigenesis and metastasis by targeting RPS4X via mTOR pathway. Theranostics **2020**;10:4627-43

15. Zoppoli G, Regairaz M, Leo E, Reinhold WC, Varma S, Ballestrero A*, et al.* Putative DNA/RNA helicase Schlafen-11 (SLFN11) sensitizes cancer cells to DNA-damaging agents. Proc Natl Acad Sci U S A **2012**;109:15030-5

16. Li M, Kao E, Gao X, Sandig H, Limmer K, Pavon-Eternod M*, et al.* Codon-usage-based inhibition of HIV protein synthesis by human schlafen 11. Nature **2012**;491:125-8

17. Stabell AC, Hawkins J, Li M, Gao X, David M, Press WH*, et al.* Non-human Primate Schlafen11 Inhibits Production of Both Host and Viral Proteins. PLoS Pathog **2016**;12:e1006066

18. Walter P, Ron D. The unfolded protein response: from stress pathway to homeostatic regulation. Science **2011**;334:1081-6

19. Tabas I, Ron D. Integrating the mechanisms of apoptosis induced by endoplasmic reticulum stress. Nat Cell Biol **2011**;13:184-90

20. Zhou HJ, Wang J, Yao B, Wong S, Djakovic S, Kumar B*, et al.* Discovery of a First-in-Class, Potent, Selective, and Orally Bioavailable Inhibitor of the p97 AAA ATPase (CB-5083). J Med Chem **2015**;58:9480-97

21. Jin J, Li X, Gygi SP, Harper JW. Dual E1 activation systems for ubiquitin differentially regulate E2 enzyme charging. Nature **2007**;447:1135-8

22. Hyer ML, Milhollen MA, Ciavarri J, Fleming P, Traore T, Sappal D*, et al.* A small-molecule inhibitor of the ubiquitin activating enzyme for cancer treatment. Nat Med **2018**;24:186-93

23. Barghout SH, Schimmer AD. The ubiquitin-activating enzyme, UBA1, as a novel therapeutic target for AML. Oncotarget **2018**;9:34198-9

24. McHugh A, Fernandes K, South AP, Mellerio JE, Salas-Alanis JC, Proby CM*, et al.* Preclinical comparison of proteasome and ubiquitin E1 enzyme inhibitors in cutaneous squamous cell carcinoma: the identification of mechanisms of differential sensitivity. Oncotarget **2018**;9:20265-81

25. Monda JK, Cheeseman IM. Dynamic regulation of dynein localization revealed by small molecule inhibitors of ubiquitination enzymes. Open Biol **2018**;8

26. Barghout SH, Patel PS, Wang X, Xu GW, Kavanagh S, Halgas O*, et al.* Preclinical evaluation of the selective small-molecule UBA1 inhibitor, TAK-243, in acute myeloid leukemia. Leukemia **2019**;33:37-51

27. Best S, Hashiguchi T, Kittai A, Bruss N, Paiva C, Okada C*, et al.* Targeting ubiquitin-activating enzyme induces ER stress-mediated apoptosis in B-cell lymphoma cells. Blood Adv **2019**;3:51-62

28. Best S, Liu T, Bruss N, Kittai A, Berger A, Danilov AV. Pharmacologic inhibition of the ubiquitin-activating enzyme induces ER stress and apoptosis in chronic lymphocytic leukemia and ibrutinib-resistant mantle cell lymphoma cells. Leuk Lymphoma **2019**;60:2946-50

29. Zhuang J, Shirazi F, Singh RK, Kuiatse I, Wang H, Lee HC*, et al.* Ubiquitin-activating enzyme inhibition induces an unfolded protein response and overcomes drug resistance in myeloma. Blood **2019**;133:1572-84

30. Murai J, Feng Y, Yu GK, Ru Y, Tang SW, Shen Y*, et al.* Resistance to PARP inhibitors by SLFN11 inactivation can be overcome by ATR inhibition. Oncotarget **2016**;7:76534-50

31. Seiler JA, Conti C, Syed A, Aladjem MI, Pommier Y. The Intra-S-Phase Checkpoint Affects both DNA Replication Initiation and Elongation: Single-Cell and -DNA Fiber Analyses. Mol Cell Biol **2007**;27:5806-18

32. Kim DI, Jensen SC, Noble KA, Kc B, Roux KH, Motamedchaboki K*, et al.* An improved smaller biotin ligase for BioID proximity labeling. Mol Biol Cell **2016**;27:1188-96

33. Yang JY, Deng XY, Li YS, Ma XC, Feng JX, Yu B*, et al.* Structure of Schlafen13 reveals a new class of tRNA/rRNA- targeting RNase engaged in translational control. Nat Commun **2018**;9:1165

34. Saldivar JC, Cortez D, Cimprich KA. The essential kinase ATR: ensuring faithful duplication of a challenging genome. Nat Rev Mol Cell Biol **2017**;18:622-36

35. Smits VAJ, Cabrera E, Freire R, Gillespie DA. Claspin - checkpoint adaptor and DNA replication factor. FEBS J **2019**;286:441-55

36. Cabrera E, Hernandez-Perez S, Koundrioukoff S, Debatisse M, Kim D, Smolka MB*, et al.* PERK inhibits DNA replication during the Unfolded Protein Response via Claspin and Chk1. Oncogene **2017**;36:678-86

37. Malzer E, Daly ML, Moloney A, Sendall TJ, Thomas SE, Ryder E*, et al.* Impaired tissue growth is mediated by checkpoint kinase 1 (CHK1) in the integrated stress response. J Cell Sci **2010**;123:2892-900

38. Thomas SE, Malzer E, Ordonez A, Dalton LE, van 't Wout EF, Liniker E*, et al.* p53 and translation attenuation regulate distinct cell cycle checkpoints during endoplasmic reticulum (ER) stress. J Biol Chem **2013**;288:7606-17

39. Wang M, Kaufman RJ. The impact of the endoplasmic reticulum protein-folding environment on cancer development. Nat Rev Cancer **2014**;14:581-97

40. Christianson JC, Ye Y. Cleaning up in the endoplasmic reticulum: ubiquitin in charge. Nat Struct Mol Biol **2014**;21:325-35

41. Bonner WM, Redon CE, Dickey JS, Nakamura AJ, Sedelnikova OA, Solier S*, et al.* gammaH2AX and cancer. Nat Rev Cancer **2008**;8:957-67

42. Solier S, Pommier Y. The nuclear gamma-H2AX apoptotic ring: implications for cancers and autoimmune diseases. Cell Mol Life Sci **2014**;71:2289-97

43. Li M, Kao E, Malone D, Gao X, Wang JYJ, David M. DNA damage-induced cell death relies on SLFN11-dependent cleavage of distinct type II tRNAs. Nat Struct Mol Biol **2018**;25:1047-58

44. Valdez F, Salvador J, Palermo PM, Mohl JE, Hanley KA, Watts D*, et al.* Schlafen 11 Restricts Flavivirus Replication. J Virol **2019**;93

45. Zhang Y, Yang Z, Cao Y, Zhang S, Li H, Huang Y*, et al.* The Hsp40 family chaperone protein DnaJB6 enhances Schlafen1 nuclear localization which is critical for promotion of cell-cycle arrest in T-cells. Biochem J **2008**;413:239-50

46. Benyair R, Ron E, Lederkremer GZ. Protein quality control, retention, and degradation at the endoplasmic reticulum. Int Rev Cell Mol Biol **2011**;292:197-280

47. Berger M, Krebs P, Crozat K, Li X, Croker BA, Siggs OM*, et al.* An Slfn2 mutation causes lymphoid and myeloid immunodeficiency due to loss of immune cell quiescence. Nat Immunol **2010**;11:335-43

48. Omar I, Lapenna A, Cohen-Daniel L, Tirosh B, Berger M. Schlafen2 mutation unravels a role for chronic ER stress in the loss of T cell quiescence. Oncotarget **2016**;7:39396-407

49. Hetz C, Saxena S. ER stress and the unfolded protein response in neurodegeneration. Nat Rev Neurol **2017**;13:477-91

50. Behrends C, Langer CA, Boteva R, Bottcher UM, Stemp MJ, Schaffar G*, et al.* Chaperonin TRiC promotes the assembly of polyQ expansion proteins into nontoxic oligomers. Mol Cell **2006**;23:887-97

Figures legends

Figure 1. SLFN11-deficient cells are hypersensitive toTAK-243.

(**A**) Isogenic leukemic lymphoblasts CCRF-CEM *SLFN11*-WT and -KO cells were screened with the indicated compounds. D1: 63.2 nM, D2: 189.6 nM. (**B-D**) TAK-243 cytotoxicity in the indicated *SLFN11*-WT and -KO isogenic cell lines: prostate cancer DU145, hepatocellular carcinoma Li-7 and leukemic lymphoblasts MOLT4. Cells were treated with the indicated concentrations of TAK-243 for 72 hours. Error bars represent SD for 3 independent experiments. (**E**) IC50 values of TAK-243 in the different cell lines shown in panels B-D. Mean ± SD and P-values are shown and statistical significance was determined by the unpaired t test. (**F**) Colony forming assay in DU145 *SLFN11*-WT and -KO cells treated with the indicated concentrations of TAK-243 for 10 days. The images of colony formation stained with crystal violet.

Figure 2. TAK-243 inhibits DNA replication more effectively in SLFN11-deficient (KO) than proficient (WT) DU145 prostate cancer cells.

(**A**) Representative flow cytometry experiment. WT and KO cells were treated with the indicated TAK-243 concentrations for 4 hours, and EdU (10 μM) was added for the last 30 min before harvesting. The percentage of replicating (EdU and DAPI positive) cells measured by FlowJo was indicated in the red boxes. (**B**) Quantitation of EdU incorporation for 3 independent experiments as shown in panel A. Error bars represent SD; ** P = 0.002, *** P < 0.001. (**C**) Representative image of EdU incorporation visualized by confocal immunofluorescence microscopy. WT and KO cells were treated with TAK-243 (0.5 μM) for 4 hours. EdU (10 μM) was added for the last 30 min. Nuclei were stained with DAPI (blue). (**D**) Quantitation of EdU incorporation in WT and KO cells from the immunofluorescence analyses. Error bars represent SD (N = 250-300). *** P < 0.001. (**E**) Inhibition of replication fork progression analyzed by molecular combing assay. Upper panel: experimental scheme. WT and KO cells were incubated with CldU (100 μM) for 1 hour before adding TAK-243 (0.5 μM) and IdU (100 μM) for 2 hours. Bottom panel: representative images of

DNA fibers. The red and green-colored part of fibers represent intake of CldU and IdU, respectively. (**F**) Ratio of IdU/CIdU (green/red). The length of the green or red-colored section of individual fibers are shown in Figure S2. Red bars represent means (N ≥ 198). *** P < 0.001. (**G**) New origins defined as ldU-single-labeled fibers measured in the DNA combing assay. Percentage was calculated from the number of green signals divided by the total number of signals (N = 177). Error bars represent SD (N = 3 independent measurements); ** P = 0.003, *** P < 0.001.

Figure 3. TAK-243 inhibits DNA synthesis through CHK1 activation, independently of ATR.

(**A**) DNA damage response (DDR) proteins detected by Western blotting after TAK-243 treatment. DU145 *SLFN11*-WT and -KO cells were treated with TAK-243 for the indicated times. WT cells treated with camptothecin (CPT 100 nM) for 4 hours served as positive control. (**B, C**) Quantitation of p-CHK1 and p-ATR for 3 independent experiments as shown in panel A. Error bars represent SD; ** P = 0.003, *** P < 0.001. (**D**) CHK1 activation by TAK-243 is independent of ATR. DU145 *SLFN11*-KO cells were treated with TAK-243 (1 μM) for 4 hours in the absence or presence of the ATR inhibitor (M-4344; 5 nM). (**E**) Quantitation of p-CHK1 for 3 independent experiments as shown in panel D. Error bars represent SD; * P = 0.042, ** P = 0.002. (**F**) siClaspin suppresses the CHK1 activation by TAK-243. DU145 *SLFN11*-KO cells were transfected with siClaspin for 48 hours before TAK-243 treatment (0.5 μM 4 hours).(**G**) Upper panel shows the experimental scheme used for flow cytometry analysis of DU145 *SLFN11*-KO cells treated with TAK-243 and the CHK1 inhibitor (LY2606368, 100 nM). EdU (10 μM) was added 30 min prior to cell harvest as indicated. Bottom panel: EdU and DAPI positive cells were quantified by flow cytometry. The percentage of replicating (EdU positive) cells (indicated in the red rectangles) was determined as in Figure 2. (**H**) Quantitation of EdU incorporation for 3 independent experiments as shown in panel G. Error bars represent SD. * P = 0.039, *** P < 0.001. (**I**) CHK1 activation by TAK-243 is suppressed by SLFN11. As indicated, SLFN11-negative 293T cells were transfected for 48 hours with SLFN11 construct before TAK-243 treatment (0.5 μM 4 hours).

Figure 4. SLFN11 KO cells have high baseline ubiquitylation and TAK-243 further reduces ubiquitin conjugates and eliciting ER stress-mediated UPR in those cells.

(**A**) Scheme of the unfolded protein response (UPR). ERAD: ER associated degradation of misfolded proteins. (**B**) Activation of the UPR response by TAK-243 (0.5 μM) was measured by Western blotting in DU145 WT and *SLFN11*-KO cells as indicated. WT cells treated with CPT (100 nM for 4 hours) served as control. (**C**) Quantitation of p-eIF2α for 3 independent experiments as shown in panel B. (**D**) Phosphorylation of eIF2α by combination of TAK-243 and the PERK-ATF4 inhibitor. Cells were treated with TAK-243 (0.5 μM) for 4 hours and the PERK-ATF4 inhibitor (ISRIB; 10 μM) was added 1 hour prior to TAK-243. (**E**) Quantitation of p-CHK1 for 3 independent experiments as shown in panel D. (**F**) Ubiquitin conjugates [(Ub)n] determined by Western blotting. DU145 cells were treated with the indicated TAK-243 concentrations for 1 hour. The red rectangle indicates the area quantified in panel G. (**G**) Quantitation of total ubiquitin conjugates after 1 hour TAK-243 treatment. The error bars represent SD (N = 6); * P = 0.031, *** P < 0.001. (**H**) Basal ubiquitin conjugates [(Ub)n] changes in doxycycline (Dox)-inducible SLFN11 expressing cells. The cells were treated with Dox 10 μg/ml for the indicated time. The red rectangle indicates the area quantified in panel I. (**I**) Quantitation of total ubiquitin conjugates after Dox treatment. The error bars represent SD (N = 2); ** P = 0.002, *** P < 0.001.

Figure 5. SLFN11 interactions with translation initiation and protein folding complexes.

(**A**) Scheme of the PROTEOSTAT® aggregated protein detection assay. (**B**) Representative image of aggregated protein in DU145 *SLFN11*-WT and KO cells with or without TAK-243 (50 nM, 24 hours) measured by flow cytometry. (**C**) Quantitation of aggregated protein as shown in panel B. The error bars represent SD (N = 5); * P = 0.013, ** P = 0.002, *** P < 0.001. (**D**) Schematic overview of the biotinylated mass-spectrometry assay and immunoblotting protocol. (**E**) Protein interaction network of SLFN11 generated by STRING analysis. Line thickness represents the strength of data confidence. (**F**) Gene ontology (GO) analysis of molecular network associated with SLFN11. (**G**) Validation of interactions with

EIF3B and CCT2. Cells were transfected with SLFN11 vector used in Figure S5E. TAK-243 (0.5 μM) was added for 4 hours prior to cell harvest. After immunoprecipitation with streptavidin, immunoblotting was performed with the indicated antibodies. (**H**) Proximity ligation assay for SLFN11 interaction with EIF3B and CCT2 in DU145 cells. The red dots indicate the protein interactions. Images were captured by Zeiss LSM 780 ELYRA (63x magnification) and modified by ImageJ software. (**I**) Quantitation of PLA intensity as shown in panel H by ImageJ software (N>100). *** $P < 0.001$ (t-test).

Figure 6. Proposed model of SLFN11-mediated protein quality control and connection with TAK-243. SLFN11 interacts with protein chaperone TRiC/CCT complex and translation initiation complex and reduces protein misfolding. TAK-243 blocks ubiquitination, promotes the accumulation of misfolded proteins and causes ER stress and uncontrolled UPR. In the absence of SLFN11, misfolded proteins accumulate leading to protein ubiquitylation, activation of ER stress and UPR. TAK-243-induced UPR hyperactivation induces CHK1 activation via Claspin.

Figure 1.

A

Inhibitor	Target	Mechanism of action	Cell viability (%) WT D1	WT D2	KO D1	KO D2
TAK-243 (MLN-7243)	UBE1	Ubiquitin-Activating Enzyme E1 Inhibitor	92	19	53	8
THZ1	CDK7	CDK7 Inhibitor	69	29	39	11
Volasertib (BI 6727)	PLK1	Polo-like Kinase-1 (Plk-1) Inhibitor	84	15	36	21
Betamethasone	NR3C1	Glucocorticoid receptor antagonist	81	56	44	23
Desonide	NA	Corticosteroid	109	84	66	57
Clofarabine	NA	DNA Polymerase Inhibitor	11	10	68	64
SN-38	TOP1	DNA Topoisomerase I Inhibitor	12	10	85	69
Camptothecin	TOP1	DNA Topoisomerase I Inhibitor	12	9	83	83
10-hydroxycamptothecin	TOP1	DNA Topoisomerase I Inhibitor	13	11	95	85
Topotecan HCl	TOP1	DNA Topoisomerase I Inhibitor	34	17	105	109

B

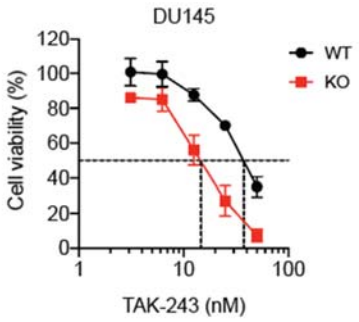

C

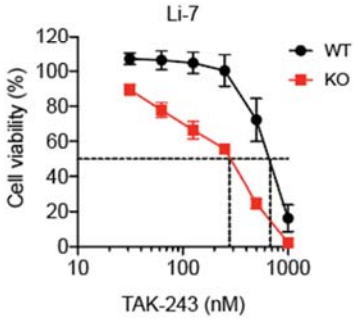

D

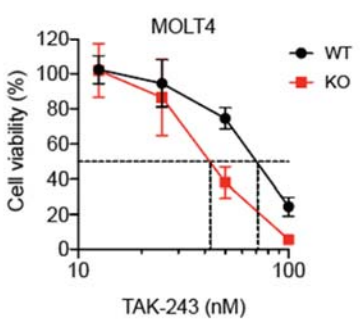

E

Cell lines	WT (IC50)	KO (IC50)	*P*-value
DU145	38.7 ± 4.1	15.6 ± 2.2	0.001
Li-7	700.1 ± 98.4	249.6 ± 11.0	0.001
MOLT4	73.9 ± 7.8	44.5 ± 8.8	0.012

F

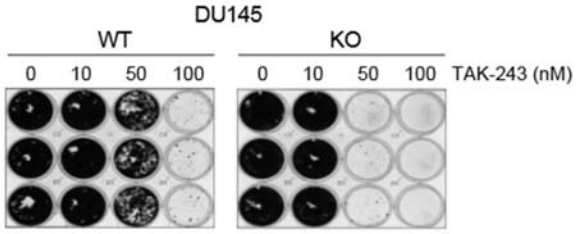

Figure 2.

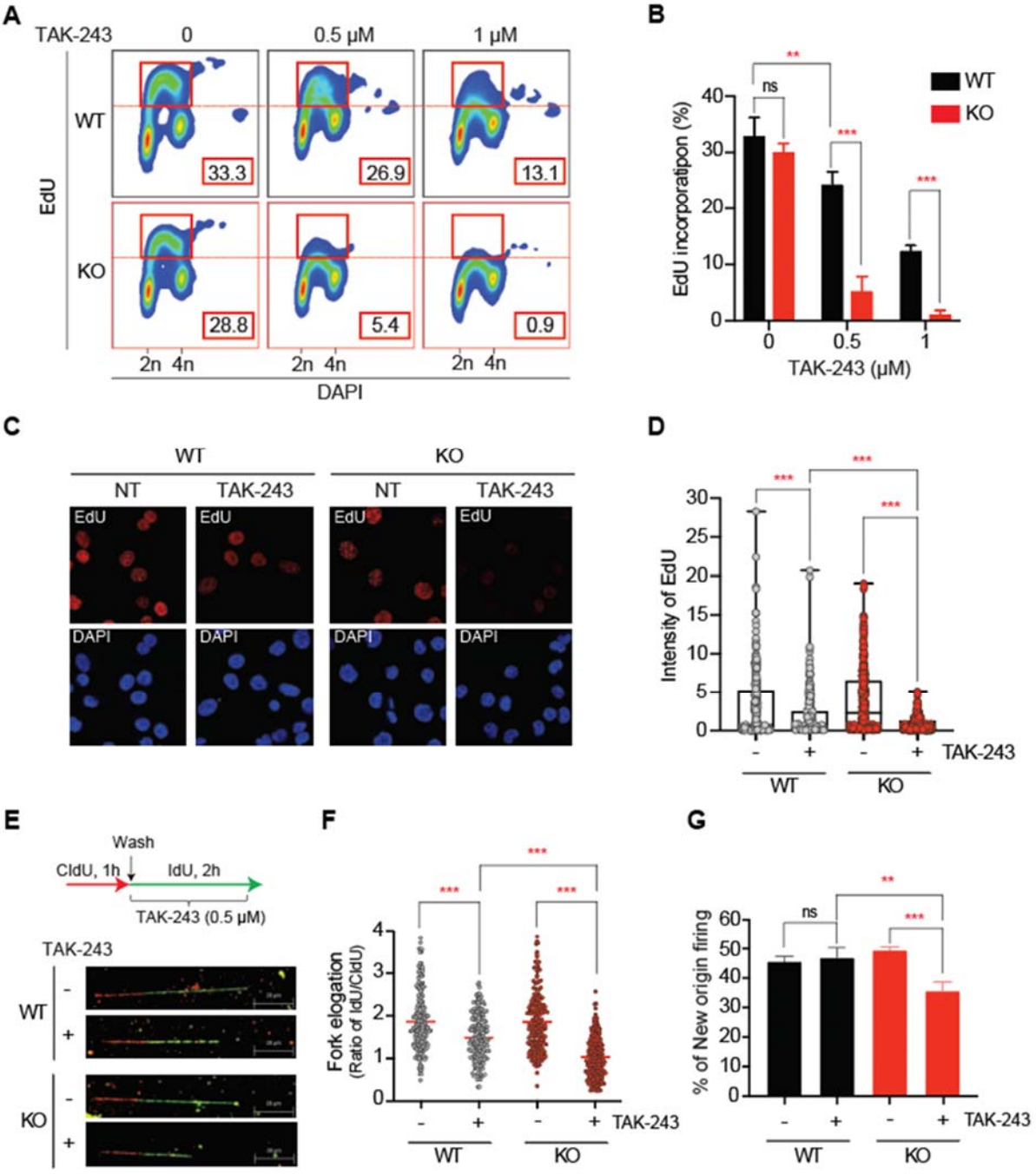
A
TAK-243
0
0.5 μM
1 μM
WT
KO
EdU
33.3
26.9
13.1
28.8
5.4
0.9
2n 4n
DAPI
B
WT
KO
ns
**
***
***
EdU incorporatipon (%)
0
10
20
30
40
0
0.5
1
TAK-243 (μM)
C
WT
KO
NT
TAK-243
EdU
DAPI
D
***
***
***
Intensity of EdU
0
5
10
15
20
25
30
-
+
-
+
TAK-243
WT
KO
E
Wash
CldU, 1h
IdU, 2h
TAK-243 (0.5 μM)
TAK-243
WT
KO
F
***
***
***
Fork elogation
(Ratio of IdU/CldU)
0
1
2
3
4
TAK-243
WT
KO
G
**
ns
***
% of New origin firing
0
10
20
30
40
50
60
TAK-243
WT
KO

Figure 3.

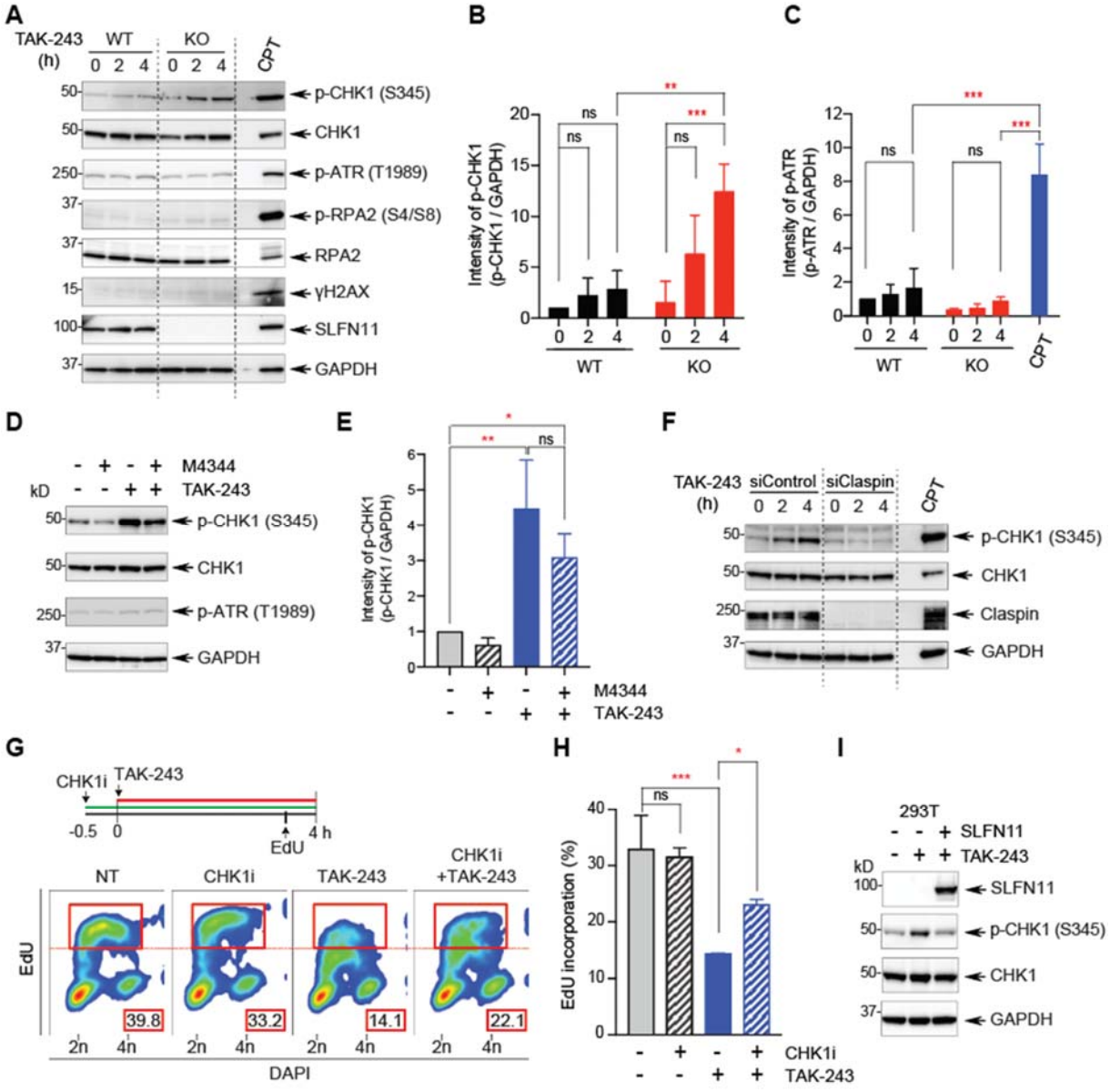
A
TAK-243
(h)
WT
KO
0 2 4 0 2 4
CPT
p-CHK1 (S345)
CHK1
p-ATR (T1989)
p-RPA2 (S4/S8)
RPA2
γH2AX
SLFN11
GAPDH
B
Intensity of p-CHK1 (p-CHK1 / GAPDH)
ns
**
***
WT
KO
C
Intensity of p-ATR (p-ATR / GAPDH)
D
M4344
TAK-243
kD
E
Intensity of p-CHK1 (p-CHK1 / GAPDH)
F
siControl
siClaspin
Claspin
G
CHK1i
TAK-243
EdU
4 h
NT
CHK1i
TAK-243
CHK1i +TAK-243
39.8
33.2
14.1
22.1
2n
4n
DAPI
H
EdU incorporation (%)
I
293T
SLFN11

Figure 4.

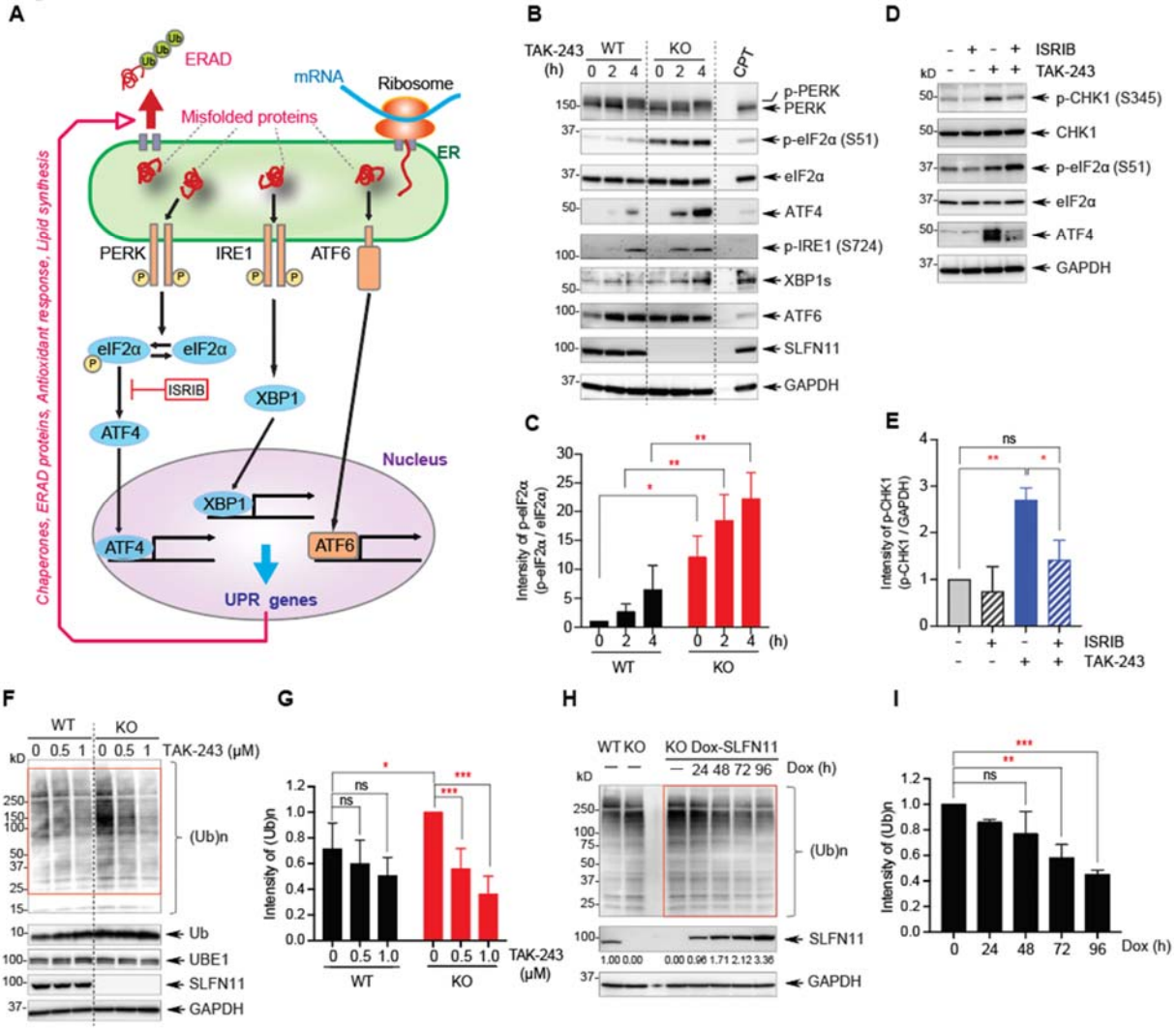
A
ERAD
mRNA
Ribosome
Misfolded proteins
ER
PERK
IRE1
ATF6
eIF2α
ISRIB
XBP1
ATF4
Nucleus
UPR genes
Chaperones, ERAD proteins, Antioxidant response, Lipid synthesis
B
TAK-243 (h)
WT
KO
CPT
p-PERK
PERK
p-eIF2α (S51)
eIF2α
ATF4
p-IRE1 (S724)
XBP1s
ATF6
SLFN11
GAPDH
C
Intensity of p-eIF2α (p-eIF2α / eIF2α)
D
ISRIB
TAK-243
p-CHK1 (S345)
CHK1
E
Intensity of p-CHK1 (p-CHK1 / GAPDH)
F
TAK-243 (μM)
(Ub)n
Ub
UBE1
G
Intensity of (Ub)n
H
WT KO
KO Dox-SLFN11
Dox (h)
I

Figure 5.

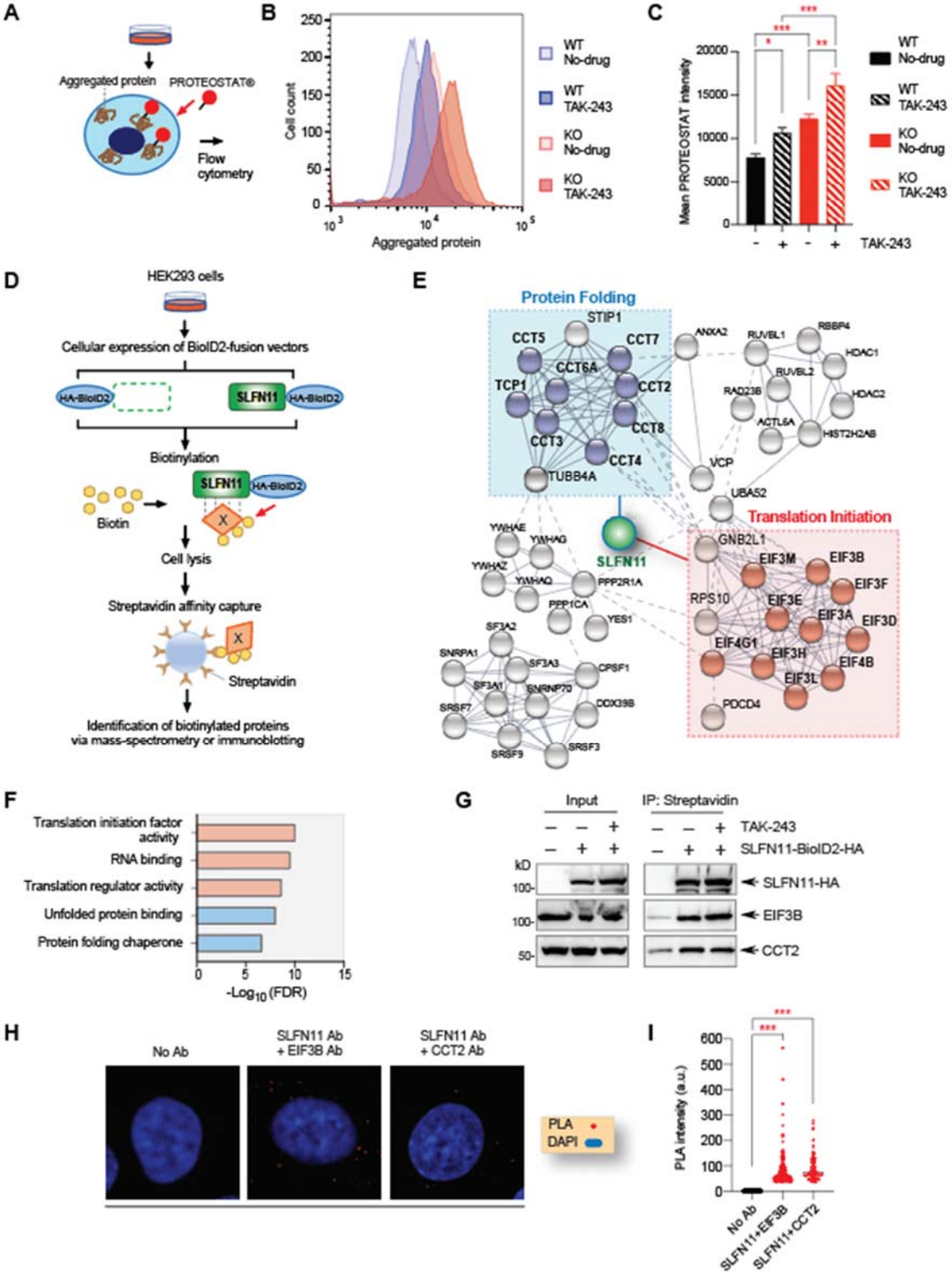
A
Aggregated protein
PROTEOSTAT®
Flow cytometry
B
Cell count
Aggregated protein
WT No-drug
WT TAK-243
KO No-drug
KO TAK-243
C
Mean PROTEOSTAT intensity
TAK-243
D
HEK293 cells
Cellular expression of BioID2-fusion vectors
HA-BioID2
SLFN11
Biotinylation
Biotin
Cell lysis
Streptavidin affinity capture
Streptavidin
Identification of biotinylated proteins via mass-spectrometry or immunoblotting
E
Protein Folding
Translation Initiation
STIP1
CCT5
CCT7
CCT6A
TCP1
CCT2
CCT8
CCT3
CCT4
TUBB4A
ANXA2
RUVBL1
RBBP4
HDAC1
RUVBL2
RAD23B
HDAC2
ACTL6A
HIST2H2AB
VCP
UBA52
YWHAE
YWHAG
YWHAZ
YWHAQ
PPP2R1A
PPP1CA
YES1
GNB2L1
EIF3M
EIF3B
EIF3F
RPS10
EIF3E
EIF3A
EIF3D
EIF4G1
EIF3H
EIF4B
EIF3L
PDCD4
SF3A2
SNRPA1
SF3A3
CPSF1
SF3A1
SNRNP70
DDX39B
SRSF7
SRSF9
SRSF3
F
Translation initiation factor activity
RNA binding
Translation regulator activity
Unfolded protein binding
Protein folding chaperone
-Log10 (FDR)
G
Input
IP: Streptavidin
TAK-243
SLFN11-BioID2-HA
kD
SLFN11-HA
EIF3B
CCT2
H
No Ab
SLFN11 Ab + EIF3B Ab
SLFN11 Ab + CCT2 Ab
PLA
DAPI
I
PLA intensity (a.u.)
No Ab
SLFN11+EIF3B
SLFN11+CCT2

Figure 6.

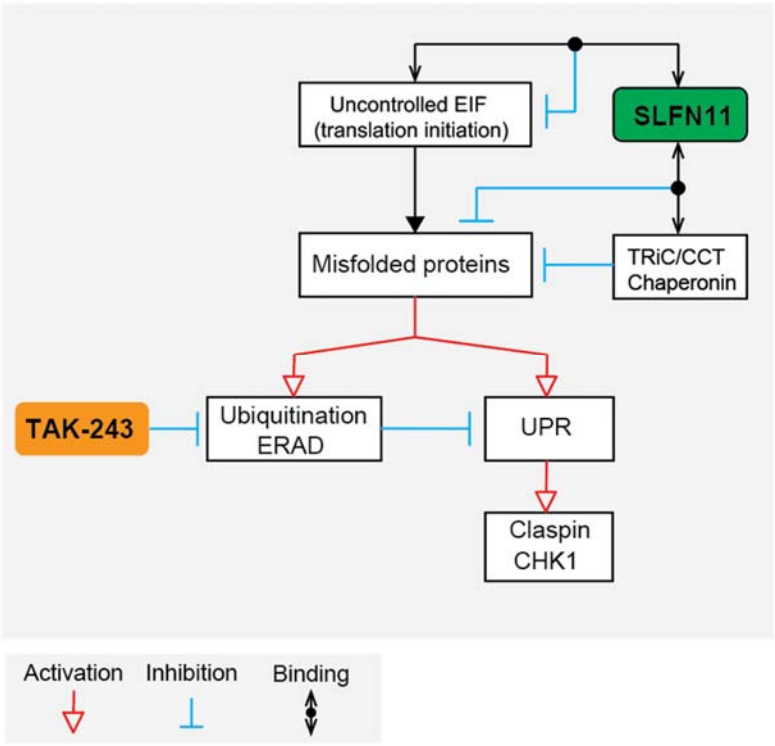
Uncontrolled EIF
(translation initiation)
SLFN11
Misfolded proteins
TRiC/CCT
Chaperonin
TAK-243
Ubiquitination
ERAD
UPR
Claspin
CHK1
Activation
Inhibition
Binding

Supplemental Figures and legends

Figure S1

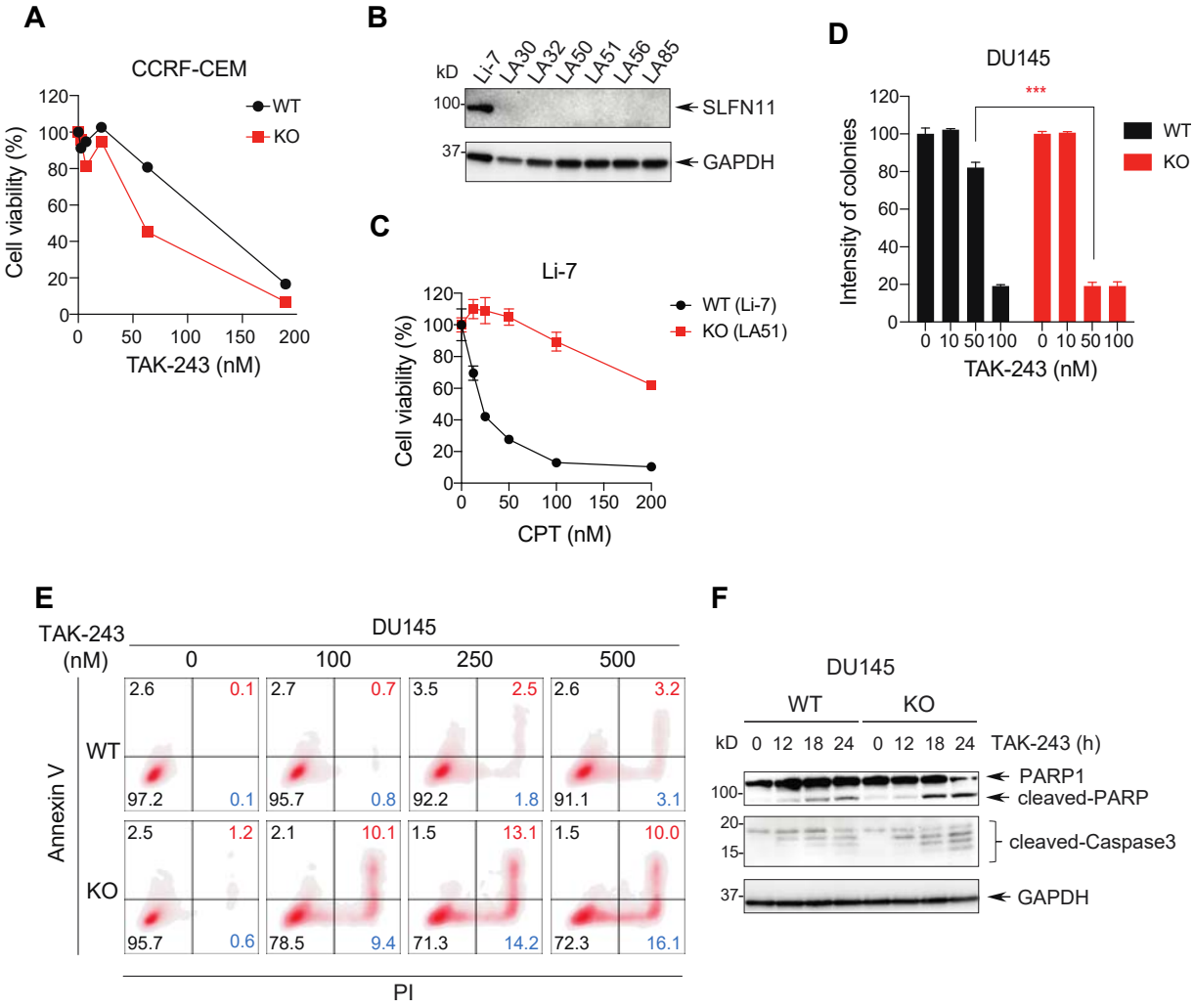

Figure S1, related to Figure 1.

(**A**) Isogenic leukemic lymphoblasts CCRF-CEM *SLFN11*-WT and -KO cells were treated with the indicated concentrations of TAK-243 in our drug screening. (**B**) *SLFN11*-KO cell lines in Li-7 were created with CRISPAR-Cas9. The protein level of SLFN11 were evaluated by Western blotting. In this study, we used the LA51 cell line as *SLFN11*-KO cells. (**C**) CPT cytotoxicity in Li-7 *SLFN11*-WT and -KO cell lines. Cells were treated with the indicated concentrations of CPT for 72 hours. (**D**) The intensity of colony forming was quantified by Image J. The error bars represent SD (N=3). Statistical significance was determined by the two-way ANOVA test and Sidak's multiple comparison test; *** $P < 0.001$. (**E**) Cellular apoptosis in DU145 *SLFN11*-WT and -KO cells was analyzed by flow cytometry after treatment with the indicated TAK-243 concentration for 24 hours. (**F**) Cleaved-PARP and cleaved-Caspase 3 in DU145 *SLFN11*-WT and -KO cells treated with TAK-243 (0.5 μM) for 24 hours were measured by Western blotting.

Figure S2

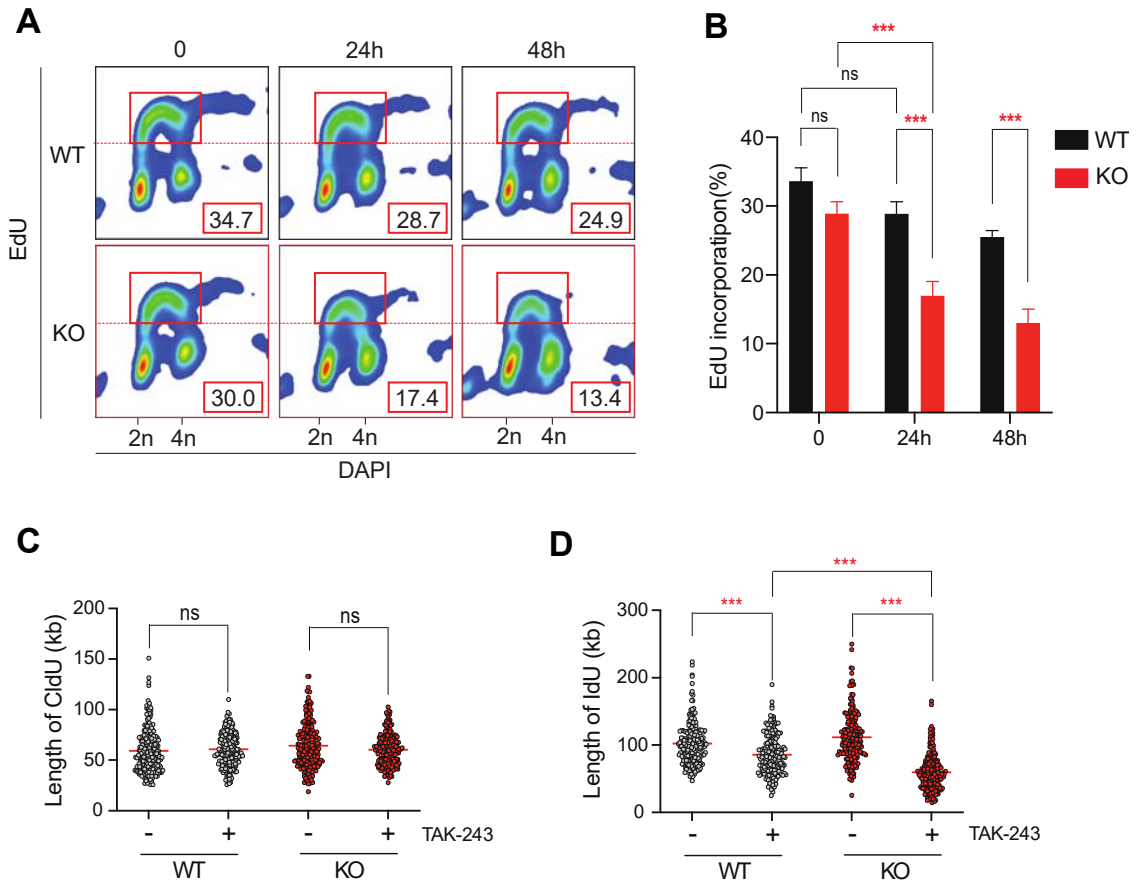

Figure S2, related to Figure 2.

(**A**) Representative flow cytometry experiment. *SLFN11*-proficient (WT) DU145 cells and *SLFN11*-deficient (KO) cells were treated with TAK-243 25 nM for 24 or 48 hours, and EdU (10 μM) was added for the last 30 min before harvesting. The percentage of replicating (EdU and DAPI positive) cells measured by Flow Jo was indicated in the red boxes. (**B**) Quantitation of EdU incorporation for 3 independent experiments as shown in panel A. Error bars represent SD; *** $P < 0.001$. (**C, D**) Fork elongation speed was calculated form ratio of IdU/CIdU(green/red) in the DNA combing assay. The length of red or green-colored part in counted DNA fibers was analyzed. Error bars represent mean ($N \geq 198$); ns; not significant, *** $P < 0.001$.

Figure S3

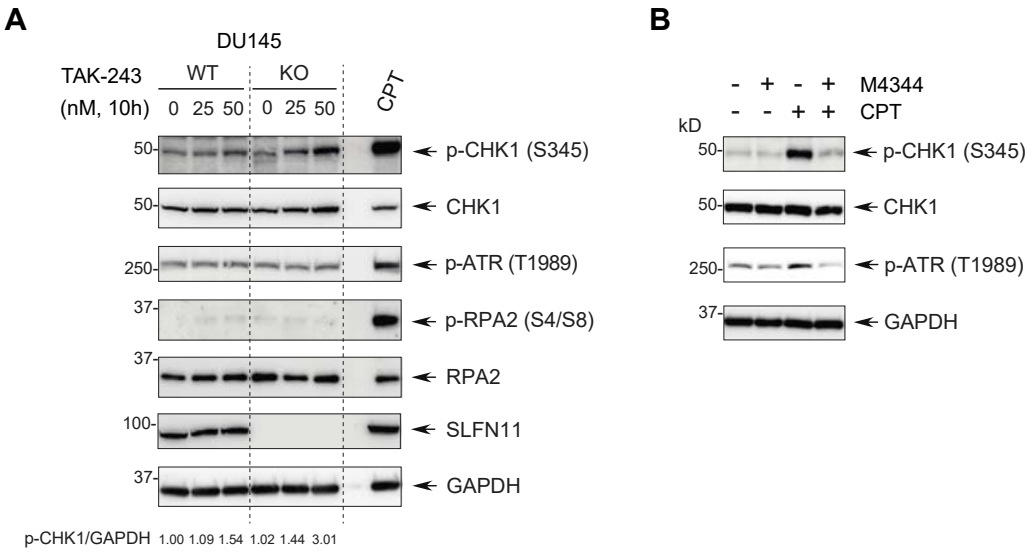

Figure S3, related to Figure 3.
(**A**) DNA damage response (DDR) proteins detected by Western blotting after TAK-243 treatment. DU145 *SLFN11*-WT and -KO cells were treated with the indicated concentrations of TAK-243 for 10 hours. WT cells treated with camptothecin (CPT 100 nM) for 4 hours served as positive control. (**B**) CHK1 activation by CPT (100 nM 4 hours) is reduced by the ATR inhibitor (M-4344; 5 nM).

Figure S4

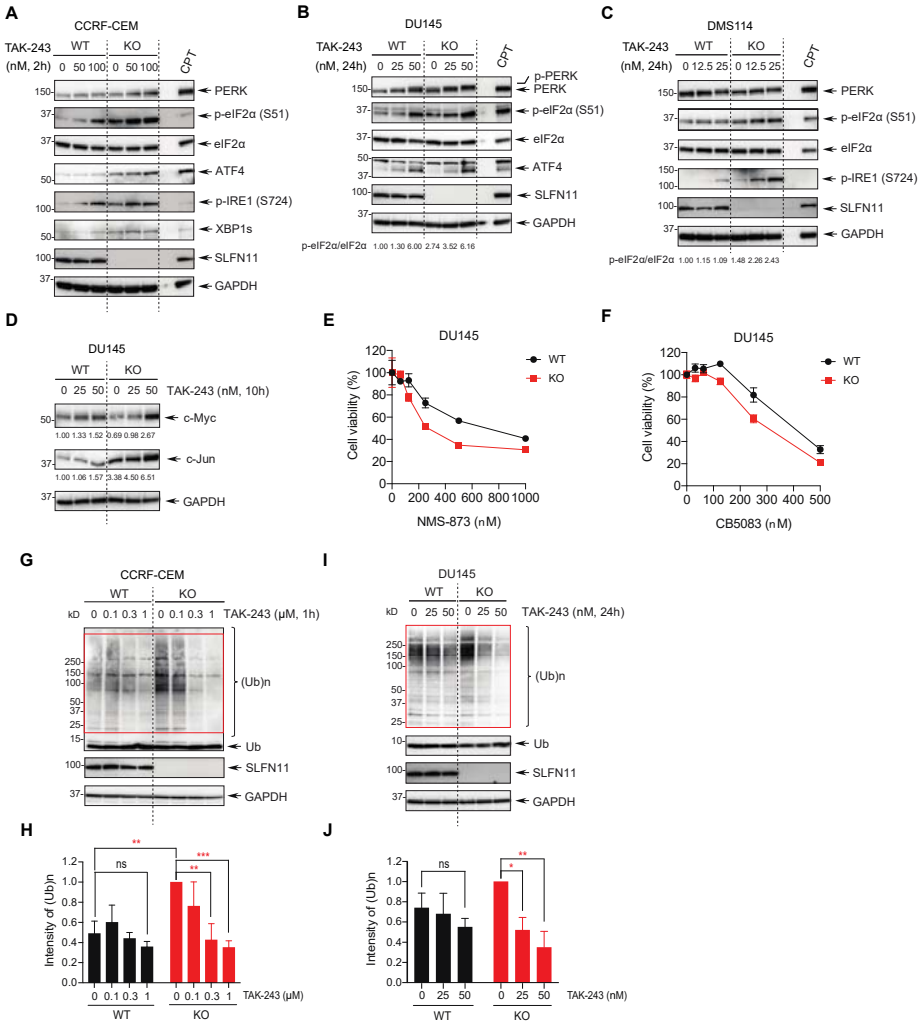

Figure S4, related to Figure 4.

(**A**) Activation of the UPR response by TAK-243 in CCRF-CEM cells was measured by Western blotting as indicated. WT cells treated with CPT (100 nM for 2 hours) served as control. (**B, C**) DU145 cells and DMS114 cells were treated with the indicated concentrations of TAK-243 for 24 hours. WT cells treated with CPT (100 nM for 4 hours) served as control. (**D**) Accumulation of short-lived proteins in TAK-243-treated cells measured by Western blotting. (**E-F**) Cell viability with p97 inhibitors in DU145 *SLFN11*-WT and -KO cells. Cells were treated with the indicated concentrations of p97 inhibitors for 72 hours. (**G**) Ubiquitin conjugates [(Ub)n] determined by Western blotting. CCRF-CEM cells were treated with the indicated TAK-243 concentrations for 1 hour. The red rectangle indicates the area quantified in panel H. (**H**) Quantitation of total ubiquitin conjugates after 1 hour TAK-243 treatment. The error bars represent SD (N = 3); ** P < 0.01, *** P < 0.001. (**I**) Ubiquitin conjugates [(Ub)n] determined by Western blotting. DU145 cells were treated with the indicated TAK-243 concentrations for 24 hours. The red rectangle indicates the area quantified in panel J. (**J**) Quantitation of total ubiquitin conjugates after 24 hours TAK-243 treatment. The error bars represent SD (N = 3); * P = 0.015, ** P = 0.001.

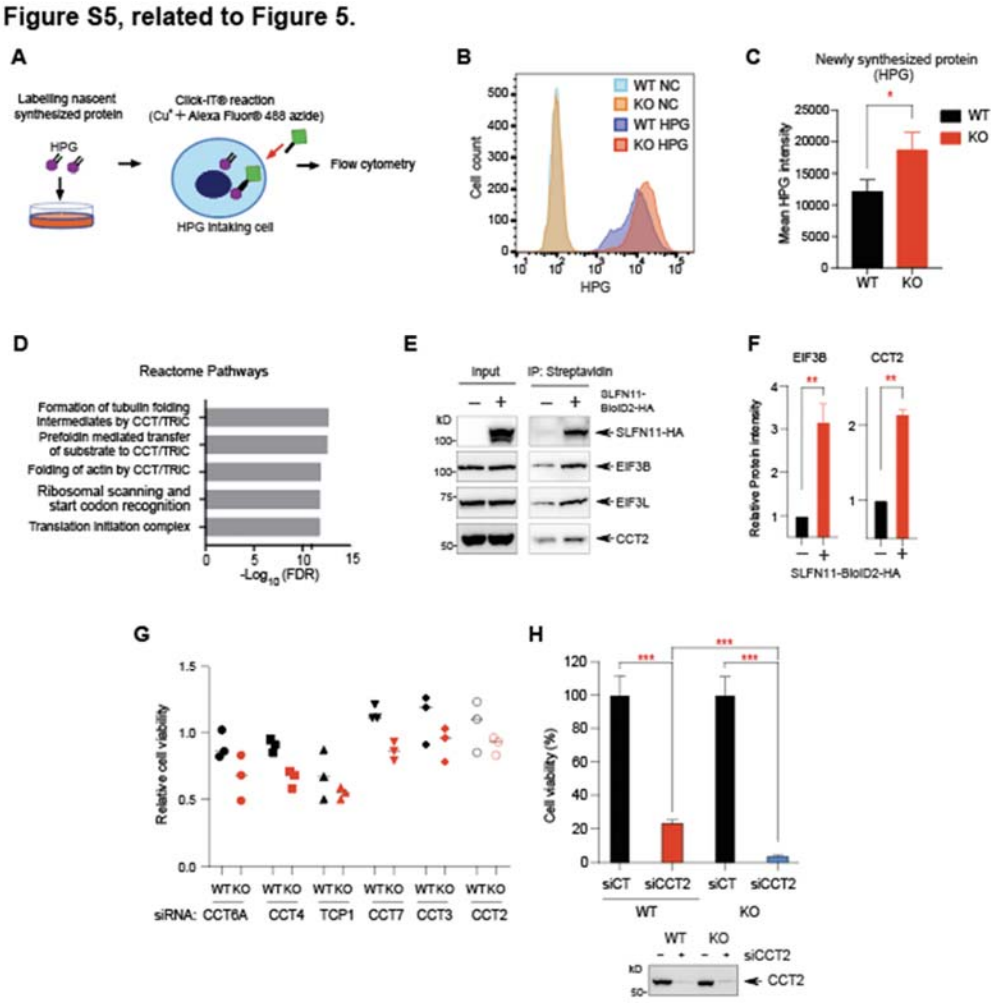

Figure S5, related to Figure 5.

(**A**) Schema of newly synthesized protein detection by L-homopropargylglycine (HPG) labelling. (**B**) Representative image of newly synthesized proteins in Li-7 *SLFN11*-WT and KO cells measured by flow cytometry. NC; negative control. (**C**) Quantitation of nascent proteins as shown in panel B. Error bars represent SD (N=3); * P = 0.031. (**D**) Gene ontology (GO) analysis of molecular network associated with SLFN11. GO enrichment is sorted by Reactome Pathway. (**E**) Validation of SLFN11 interactions with the indicated translation initiation (EIF3B and EIF3L) and protein folding (CCT2) factors. Following transfection with SLFN11-BioID2-HA or Empty vector as indicated in Figure 5D, cell lysates were immunoprecipitated with streptavidin and immunoblotting performed with the indicated antibodies. (**F**) Quantification of EIF3B and CCT2 for repeated experiments as shown in panel E. Error bars represent standard error of the mean; EIF3B (N=3) ** P = 0.007, CCT2 (N=2) ** P = 0.003. (**G**) Relative cell viability between DU145 *SLFN11* WT and KO cells with gene depletion of the TRiC/CCT chaperonin complex in RNAi screening (Supplementary Table 3). Genes were silenced by transfection with 3 independent siRNAs. (**H**) Cell viability after transfection with siCCT2 in DU145 *SLFN11* WT and KO cells. Cells were cultured with the siRNAs for 96 hours. Cell viability was analyzed by CellTiter-Glo Assay. *** P < 0.001. Gene depletion of CCT2 by siRNA transfection was determined by Western blotting.

Supplementary Materials and Methods

Colony forming assay

DU145 and DD9 (*SLFN11*-knockout) were seeded in 12-well plates. After 24-hours, TAK-243 was added and incubated for 10 days. Cells were washed with PBS, fixed and stained with 0.05% (w/v) crystal violet solution in methanol for 2 hours. Colony-stained images were taken using ChemiDoc™ Touch MP (17001402; BioRad) and analyzed by ImageJ software (NIH).

Apoptosis assay

Cells were seeded in 6-well plates and treated with TAK-243. After cell harvest, apoptotic cell death was determined by using the ApoDETECT Annexin V-FITC Kit (331200; Invitrogen) according to the manufacturer's instructions. Florescent signals were analyzed by a FACS Canto and FlowJo.

Complementation of wild-type SLFN11

Human SLFN11 cDNA was acquired from the Plasmid (HsCD00082389; Dana-Farber/Harvard Cancer Center DNA Resource Core). The full-length of SLFN11 cDNA was PCR-amplified with primers (Supplemental Table 1) and subcloned into pcDNA3 by using HindII and ApaI restriction enzyme sites. The pcDNA3-SLFN11-Flag construct is transiently transfected into 293T cells by using GeneJuice (70967; Millipore) for 48 hours.

Establishment of doxycycline-inducible SLFN11 expressing cells

DU145 *SLFN11* KO cells were plated in 6-well plates. After 24 hours, cells were infected with 500 µl of virus containing pLVX-TetOne-blasticidin-3XFlag-SLFN11. After 48 hours post-infection, cells were re-plated with blasticidin (10 µg/ml) (Gibco) for 48 hours and then single clone cell was selected by the serial-dilution method in 96-well plates.

Proximity ligation assay

Cells were plated in 4-well Nunc™ Lab-Tek™ II CC2™ Chamber Slide System (154917; Thermo Fisher) and grown for 24 hours. Following fixation with 4% PFA and permeabilization in 0.3% Triton X-100/1xPBS, cells were then applied to Duolink™ In Situ Red Starter Kit Mouse/Rabbit (DUO92101, Sigma) according to manufacturer's instructions. Briefly, cells were incubated in blocking buffer and incubated with anti-SLFN11 antibody and either rabbit anti-EIF3B and rabbit anti-CCT2 for 1 hour at room temperature. Cells were then incubated with PLUS and MINUS PLA probes for 1 hour at 37 °C. Cells were subsequently incubated with PLA ligase for 30 min at 37 °C, following by amplification with PLA polymerase for 100 min at 37 °C. Finally, cells were mounted with the Duolink In-Situ Mounting Medium with DAPI. Fluorescence signals were visualized by Zeiss LSM 780 ELYRA (63x magnification) and analyzed by ImageJ software.

RNAi screening

RNAi screening was performed by the Silencer Select Human Druggable siRNA library (Thermo Fisher) as detailly described in previous report (1). Briefly, DU145 *SLFN11* WT and KO cells were transfected with siRNAs per gene in 384-well plates, one siRNA per well. After 96 hours post-transfection, cell viability was measured with CellTiter-Glo Assay kit with BMG Pherastar plate reader. Quality control using Z' was applied in order to exclude plates with poor performance. All plates were subject to visual inspection to further remove technical errors. Viability was normalized to the negative control siRNA #2 (Thermo Fisher). The gross off targeting of an siRNA was computed as the weighted sum of all off target effects that the given siRNA could potentially be associated with. Then this gross off-target contribution was subtracted from the experimental Z-score to form the on-target Z-score. The gene-level Z-scores were calculated using the median corrected on-target Z-score. Relative Z-scores for gene-dependency between WT and KO cells were calculated by a subtraction of viability (siRNA X in *SLFN11* WT - siRNA X in *SLFN11* KO). We considered those with gene-level Z-scores < -2, or > 2 as the potential hits which are gene-dependent in *SLFN11* WT and KO cells, respectively.

1. Jo U, Murai Y, Chakka S, Chen L, Cheng K, Murai J*, et al.* SLFN11 promotes CDT1 degradation by CUL4 in response to replicative DNA damage, while its absence leads to synthetic lethality with ATR/CHK1 inhibitors. Proc Natl Acad Sci U S A **2021**;118